The BTB-ZF transcription factor Tramtrack 69 shapes neural cell lineages by coordinating cell proliferation and cell fate.

Françoise Simon[1], Anne Ramat[&], Sophie Louvet-Vallée[2], Angélique Burg[2], Agnès Audibert[2#] and Michel Gho[1#].

[1] CNRS, IBPS, UMR 7622, Laboratory of Developmental Biology, Paris F-75005, France.
[2] Sorbonne Université, UMR 7622, Laboratory of Developmental Biology, Paris F-75005, France.
[&] Present address: Department Genetics and Development, Institut de Genetique Humaine, Montpellier, France.
[#] These authors share senior authorship.

Abstract

The equilibrium between cell divisions that maintains stem cell fates and terminal cell divisions in which daughter cells adopt post-mitotic fates is essential to assure the correct number of determined cells at a given time at a given place. Here, we show that Tramtrack-69 (Ttk69, a BTB-ZF transcription factor ortholog of the human PLZF factor) plays an essential role in controlling the balance between cell proliferation and cell fate determination. In the Drosophila bristle cell lineage, we show that Ttk69 (1) promotes cell-cycle exit by downregulating the expression of *cycE*, the cyclin involved in S-phase entry, and (2) regulates terminal cell fate acquisition by downregulating that of *hamlet* and upregulating that of *Suppressor of Hairless*, two transcription factors involved in neural-fate acquisition and accessory-cell differentiation, respectively. Thus, Ttk69 plays a central role in shaping neural cell lineages by integrating molecular mechanisms that regulate progenitor cell-cycle exit and cell-fate commitment.

Introduction

Organisms are composed of morphologically and functionally distinct cell types. Such cell diversity is generated from a restricted set of precursor cells producing a limited number of differentiated cells. Division of precursor cells gives rise to daughter cells that differentiate and acquire specific fates. The transit from a proliferative to cell-cycle arrested state during this process is tightly regulated and requires changes in transcriptional programs. Disentangling the molecular mechanisms that control the balance between proliferation and differentiation is essential for understanding the formation and maintenance of organisms, as well as human diseases, such as cancer, in which this process is disturbed.

BTB-ZF transcription factors are involved in a wide variety of biological processes (Kelly and Daniel, 2006). They include *Drosophila* Broad-complex factors (BR-C), Bric-à-brac (Bab), and several pox virus zinc-finger proteins (Chaharbakhshi and Jemc, 2016). All possess a protein/protein interaction motif (BTB/POZ) at the N-terminus that allows protein homo and multimerization and one or several zinc-finger DNA-binding motifs (Bonchuk et al., 2011). These proteins are conserved from *Saccharomyces cerevisiae* to *Homo sapiens* and act as transcriptional repressors or activators, depending on the BTB domain (Siggs and Beutler, 2012). The founding BTB-ZF members are all *Drosophila* transcriptional repressors that regulate processes such as metamorphosis, ovary development, and neurogenesis (Karim et al., 1993; Sahut-Barnola et al., 1995; Siggs and Beutler, 2012). In vertebrates, the human BTB-ZF, promyelocytic leukemia zinc finger (PLZF), acts as a tumor-suppressor by maintaining cell growth inhibition and quiescence by transcriptional repression of the *c-myc* proto-oncogene (McConnell et al., 2003). Accordingly, *plzf* loss of function has been correlated with prostate and lung cancer (Jin et al., 2017). Moreover, this factor regulates organogenesis by controlling the balance between self-renewal and differentiation of neural stem cells (Gaber et al., 2013; Sobieszczuk et al., 2010). Overall, BTB-ZF proteins have fundamental and conserved roles during development, controlling cell proliferation and differentiation.

The *Drosophila* ortholog of PLZF, Tramtrack (Ttk), also plays multiple roles during development, including cell proliferation and cell-fate decisions in the nervous system, intestinal stem cells, photoreceptors, and tracheal cells (Araujo et al., 2007; Badenhorst et al., 2002; Giesen et al., 1997; Lai and Li, 1999; Liu et al., 2016; Wang et al., 2015). In particular, Ttk is a key regulator of cell fate in the peripheral nervous system, in which it promotes non-neural instead of neural fates (Guo et al., 1995). Ttk is considered to be a transcriptional

repressor from the initial studies on *even skipped* and *fushi tarazu* genes (Brown et al., 1991; Harrison and Travers, 1990). The *ttk* locus encodes two proteins, Ttk69 and Ttk88, via alternative splicing (Read and Manley, 1992). Both isoforms share a common conserved N-terminal BTB/POZ domain but contain divergent C-terminal zinc-finger C2H2-type domains for DNA binding, conferring specific DNA binding and probably independent functions for each isoform. Both have specific functions during development, although Ttk69 appears to have a broader spectrum of functions than Ttk88 (Read and Manley, 1992; Zollman et al., 1994). For example, during eye development, Ttk69, but not Ttk88, is expressed in all photoreceptor cells during the pupal stage and promotes specific non-neuronal fates, such as cone cells (Lai and Li, 1999). Similarly, Ttk69, but not Ttk88, is expressed in the embryonic nervous system, where it is required for proper glial cell development (Giesen et al., 1997). In the intestine stem cell lineage, *ttk69* loss of function leads to re-specification of enteroblasts into enteroendocrine cells, whereas *ttk88* loss of function has no phenotype (Wang et al., 2015). In addition to its well-known role in cell identity, Ttk has been also shown to be involved in cell-cycle regulation. More precisely, it has been shown that overexpression of Ttk69, but not Ttk88, causes the complete loss of mitosis in the eye disc morphogenetic furrow through the repression of the expression of String, the positive regulator of the G2/M transition (Baonza et al., 2002). Similarly, a significant increase of mitotic cells is observed in intestinal *ttk69* mutant clones, indicating that Ttk69 negatively regulates intestinal stem-cell proliferation (Wang et al., 2015). Altogether, these data highlight the essential role of Ttk69, but not Ttk88, on the control of cell proliferation and the acquisition of cell fate. In mechanosensory organs, the loss of both Ttk isoforms leads to complete transformation of sensory cells into neurons (Guo et al., 1995). Such extreme cell transformation prevents further studies to reveal elusive effects of Ttk proteins on cell fate determination and other biological processes, such as cell differentiation and cell proliferation. Indeed, our previous studies have shown that the loss of Ttk69 alone also induces cell proliferation (Audibert et al., 2005). This suggests that the study of mutations affecting specific *ttk69* transcripts may reveal cryptic roles of Ttk69 that are hidden when analyzing complete loss of function mutations. Here, we thus focus on how Ttk69 controls the balance between cell proliferation and the acquisition of cell fate in the bristle system.

The *Drosophila* external mechanosensory organs, or bristles, are an excellent model system to study the balance between proliferative and determined states of progenitor cells (Fichelson et al., 2005). Each bristle is composed of a shaft and an annular cuticular structure,

called the socket, at its base. At the cellular level, only four specialized cells, with a common origin, compose this comparatively simple structure: two outer cells, the socket and shaft cells, and two inner cells, the neuron and sheath cell (Hartenstein and Posakony, 1989). Each cell differs from the other by its size, relative position, and expression of specific markers (Figure 1A). They arise from the division of a primary precursor cell (or pI) after a stereotypical sequence of four asymmetric cell divisions (the bristle cell lineage). In the dorsal thorax, pI cells divide to generate a posterior secondary precursor cell (pIIa) and an anterior secondary precursor cell (pIIb). The division of pIIa leads to the formation of the outer cells (the pIIa sub-lineage), whereas the pIIb cell gives rise to the inner cells (the pIIb sub-lineage), following two rounds of division. First, pIIb divides to give rise to a glial cell that enters apoptosis shortly after birth and a tertiary precursor cell, pIIIb. Then, pIIIb divides to produce the sheath and the neuron (Fichelson and Gho, 2003; Gho et al., 1999). At each of these divisions, the Notch (N) pathway is differentially activated in only one daughter cell. This differential activation ensures the acquisition of different fates by both daughter cells (Guo et al., 1996). As such, the N-pathway does not specify particular identities, but its activation triggers different outcomes depending on the cellular context, likely in cooperation with other factors that specify cell fate (Ramat et al., 2016). Only some of these specific factors are known in the bristle lineage. Two are Sequoia (Seq) and Hamlet (Ham), two zinc-finger transcription factors, expressed in pIIb sub-lineage cells, that have a critical role in the acquisition of inner cell identity (Andrews et al., 2009; Moore et al., 2002; Moore et al., 2004). Indeed, sensory organs in *ham* mutants are composed of external cells only, due to re-specification of the inner cells. Similar cell identity transformation is also observed in *seq* mutant organs, in which neuron and sheath cells are transformed into socket and shaft cells, respectively. Moreover, it has also been shown that Seq controls *ham* expression, indicating that these factors are related in a complex regulatory network of transcription factors (Andrews et al., 2009).

Here, we use the bristle lineage to explore how Ttk69 coordinates terminal cell determination and cell-cycle arrest. We show that loss of *ttk69* leads to the production of supernumerary progenitor cells and the re-specification of cell fate identity. Notably, we observed a cousin-cousin cell transformation in which the presumed outer cell precursor acquired an inner cell precursor identity. We identify the *cycE* gene, encoding the essential cyclin required for entry into S-phase, as a transcriptional Ttk69 target. In addition, we show that Ttk69 regulates cell-fate acquisition and terminal differentiation by controlling the

expression of *ham* and *Suppressor of Hairless* (*Su(H)*), which encodes the transducing transcription factor of N-receptor signaling. We propose that Ttk69 is a central node of a transcriptional regulatory network that assures cell lineage completion by controlling the acquisition of terminal cell fates and the arrest of cell proliferation.

Results

Ttk69 loss of function leads to the formation of sensory organs with extra inner cells and only one type of outer cell

To precisely determine the involvement of Ttk69 in cell-cycle progression and cell-fate determination, we studied somatic clones ttk^{le11}, which specifically disrupts Ttk69, hereafter called Ttk69 clones (Lai and Li, 1999). Sensory organs inside Ttk69 (called Ttk69 mutant sensory organs) were devoid of the shaft and presented only sockets externally (Figure 1B). At the cellular level, 82% (n = 30) of the mutant organs were composed of more than four cells (up to eight cells) at 28 h after pupal formation (APF), when the normal bristle linage is completed (Figure 1C arrowheads and F). Among the sensory organ cells, one (67%) or two (33%) cells were Pdm1-positive outer cells (n = 30) and, in all cases, they expressed Su(H), a landmark of socket cells (Figure 1D and F). These data show that the absence of the shaft structure is associated with the lack of a cell expressing a shaft signature (Pdm1 positive, Su(H) negative). The sockets, although present, did not have a normal shape (Figure 1B). It was previously shown that the expression of the Notch transcription factor Su(H) is first induced in presumptive socket cells in response to the N-pathway and subsequently boosted via its binding to a 3'-enhancer (ASE5, Liu and Posakony (2014)). Such auto-activation is required for normal socket-cell differentiation (Barolo et al., 2000). Su(H) expression in Ttk69 socket cells was weak, suggesting that Su(H) amplification had not occurred (compare Su(H) accumulation in control socket cells, arrows, with Ttk69 mutant socket cells, arrowhead, Figure 1H, H'). Using a ASE5::GFP reporter, we failed to detect a GFP signal in Ttk69 mutant socket cells (Figure 1H"). These data show the Su(H) auto-amplification is impaired in a Ttk69 mutant background. Thus, although Ttk69 appears to not be involved in socket cell determination, it is involved in the terminal differentiation of these cells by controlling the Su(H) auto-regulatory loop.

The remaining cells in Ttk69 mutant sensory organs expressed inner-cell markers. Immunostaining against ELAV and Prospero (Pros) revealed the presence of one to four neurons and one or no sheath cell (Figure 1E). We also observed up to three cells per cluster

that were positive for both ELAV and Pros immunostaining (Figure 1E and G). This suggests the presence of either additional pIIIb precursor cells or post-mitotic cells in which the fate was not yet well resolved or not at all (Ramat et al., 2016). Thus, the Ttk69 mutant lineage is probably not yet completed 28h APF. Overall, these data show that loss of function of Ttk69 leads to the formation of sensory organs composed of extra-inner cells and only socket cells as the outer cell type.

Ttk69 promotes cell-cycle arrest and triggers terminal cell-fate identities

Several non-exclusive explanations can account for the presence of sensory organs with supplementary cells in Ttk69 mutant sensory organs. One is that the glial cells do not die but divide and produce extra terminal cells. We examined this possibility by studying cell death in Ttk69 mutant sensory organs. TUNEL assays showed that glial cells undergo apoptosis in Ttk69 mutant sensory organs at the same time as in control organs located outside the mutant clone (Figure 2A). Thus, the supplementary cells do not originate from glial cells that resume proliferation. It is also possible that supplementary cells arise from bristle cells that do not properly exit from the cell cycle and continue to proliferate. We explored this possibility by searching for metaphasic cells using phospho-ser10 histone-3 (PH3) immunoreactivity at 28 h APF, when control sensory organ cells are already post-mitotic. Ttk69 mutant sensory organs containing four or more cells harbored sensory cells positive for PH3 (Figure 2B, arrowheads). As these clusters contained the terminal number of cells, these data show that the metaphasic cells were not due to delayed divisions. Thus, these data indicate that Ttk69 mutant sensory organs harbor supplementary cells due to additional mitoses.

We used a combination of live imaging and immunolabeling to follow the entire pattern of cell divisions in Ttk69 mutant sensory organs to unambiguously define the origins of the supernumerary cells. During time-lapse recording, sensory cells were identified by the expression of GFP under the control of the *neuralized* promoter (*neur*-GFP). At the end of each recording, the imaged notum was fixed and immunolabeled with anti-Su(H), as well as anti-ELAV and anti-Pros to highlight outer and inner cells, respectively. Imaged sensory organs could be unambiguously recognized within the fixed nota by their relative position with respect to the midline, the position of the macrochaetae, or the rows of microchaetae (Fichelson and Gho, 2004). We confirmed the presence of extra cell divisions and revealed an unexpected cell transformation event. First, there was a supplementary division in a pIIa daughter cell, identified as the future socket cell by its position in the cluster (Figure 2D,

panels 4 and 5). This extra division was symmetric, leading to two Su(H)-positive socket cells (Figure 2E). We also observed socket cells in mitosis, identified by Su(H) and PH3 immunoreactivity, in fixed material (Figure 2C, arrowhead). Thus, future socket cells undergo an extra division in the absence of Ttk69 (Figure 2F). In addition, the anteriorly located pIIa daughter cell, the presumptive shaft cell that normally does not divide, underwent repetitive cell divisions (Figure 3A, panels 3 and 5). Surprisingly, immunostaining of the resulting clusters showed that cells arising from these extra divisions acquired a neural fate, as they expressed Pros and ELAV (Figure 3B), two markers expressed in sheath and neuron cells, respectively. This suggests that presumptive shaft cells underwent cousin-cousin cell transformation in which outer cells acquired an inner cell fate. Consistent with this possibility, we also observed cells with weak expression of Pdm1 associated with weak expression of Pros in fixed material, suggesting that they were midway through transformation (arrowhead in Figure 3D, D', D"). Furthermore, we detected clusters harboring two Pros-positive cells, of which one was dividing (PH3 positive, arrowhead in Figure 3E, E', E"). These different lines of evidence led us to conclude that the presumptive shaft cells underwent cell fate re-specification and acquired a pIIIb precursor cell identity (Figure 3C). We never observed cell lineages in which both pIIa daughter cells entered division in *in vivo* recordings. This is likely due to the low probability of such cases. We do not favor the possibility that the division of pIIa daughter cells is mutually exclusive, as we observed sensory organs composed of more than five cells and harboring two socket cells, a situation that required ectopic division of both pIIa daughter cells.

The socket cells divided once, even though they were already committed to differentiate. This suggests that Ttk69 is directly involved in cell-cycle arrest, because this extra mitosis was not associated with a change in cell fate. This supplementary socket-cell division is not sufficient to explain the number of inner-cells observed in Ttk69 mutant organs. The re-specification of presumptive shaft cells into inner precursor cells can explain, in part, the observation that Ttk69 mutant sensory clusters harbored up to six neural (ELAV/Pros positive) cells, showing that extra inner-cells originate at the expense of outer cells. Overall, these results suggest that Ttk69 promotes cell precursor exit, acting both by arresting cell proliferation and triggering terminal cell fate identity.

Ttk69 induces cell cycle exit via transcriptional repression of *cycE* expression.

Our results show that Ttk69 loss of function leads to extra-mitoses, suggesting that Ttk69 regulates cell proliferation. We have already shown that Ttk69 mutant sensory cells strongly accumulate CycE protein (Audibert et al., 2005). We studied whether supplementary mitosis related to the accumulation of ectopic CycE by assessing whether a reduction in the dose of CycE could revert the phenotype of supplementary cell divisions observed in Ttk69 mutant sensory organs. As already described, we observed that most sensory organs inside Ttk69 mutant clones contained more than the normal four cells (85%, n = 37, Figure 4A). This dropped to 18% when the clones were induced in a $cycE^{AR95/+}$ heterozygous background (n = 32). In another set of experiments to study the number of socket cells, 45% of Ttk69 mutant sensory organs harbored duplicated Su(H)-positive socket cells (n = 55), whereas only 11% did so in the $cycE^{AR95/+}$ heterozygous background (n = 51). These results show that reducing the dose of CycE is sufficient to markedly reduce the number of supplementary divisions observed in Ttk69 mutant sensory organs. This strongly suggests that the supplementary mitoses observed in Ttk69 mutant sensory organs are mainly driven by the increase in CycE levels induced after Ttk69 loss of function.

We analyzed the role of Ttk69 in the transcriptional expression of *cycE* by first testing the capacity of *cycE* promotor fragments to direct *lacZ* gene expression in sensory cells (Figure 4B). It has been previously shown that a 4.6 Kb proximal fragment of the whole 16.4 Kb *cycE* promoter is able to recapitulate *cycE* expression in the embryonic peripheral nervous system (Jones et al., 2000). We tested whether the similar promoter fragment controls CycE expression in adult bristle sensory cells. Indeed, we observed β-Gal accumulation in inner cells, whereas it was only barely detected in pIIa daughter cells (Figures 4C, C' and D, D' arrows and Figure S1B and C). This expression pattern was similar to that observed for *cycE* expression under control conditions (Audibert et al., 2005). In Ttk69 mutant sensory organs, the expression of both the 16.4 and 4.6 Kb *cycE* promoter-*lacZ* constructs was upregulated. We observed a particularly high level of β–Gal accumulation in both pIIa daughter cells (Figure 4 C, C' and D, D' arrowheads). These results indicate that Ttk69 represses *cycE* expression at the transcriptional level. To accurately define which part of the *cycE* promoter is required for Ttk69 regulation, we divided the 4.6Kb-*cycE* *cis*-regulatory fragment into four regions (A to D) and monitored the regulatory activity of constructs with these regions deleted or mutated in bristle sensory cells (Figures 4B and S1A). All constructs were inserted at the same locus (using ΦC31 integrase-based tools) to avoid expression variations due to genomic environment. Eight AGGAC canonical Ttk binding sites have been identified in the 4.6 Kb

fragment: three in region A and five in region C (Brown et al., 1991; Harrison and Travers, 1988; Read and Manley, 1992). Surprisingly, deletion of both promoter regions (ΔAC) or specific substitutions of these eight binding sites by a an ACTGC sequence (ACm) did not modify the expression pattern of these transcriptional reporters in wildtype sensory organs (Figures 4E, E' and S1D, D' and E, E'). This indicates that the A and C regions are not involved in Ttk69-mediated repression of *cycE* expression. Moreover, expression of the ACm-lacZ construct was still upregulated in *Ttk69* mutant sensory organs (Figure 4E, E', arrowheads), showing that Ttk69-mediated repression of *cycE* expression in sensory cells is not mediated through the canonical AGGAC Ttk-binding sites present in the A and C regions. Thus, we focused on regions B and D. A *cycE* promoter construct bearing a deletion of region B (ΔB) showed an expression pattern similar to that of the 4.6Kb-lacZ construct, showing that the deletion of region B did not remove the Ttk69 regulatory domain (Figure S1F, F'). In contrast, deletion of region D (ΔD-lacZ) led to high levels of βGal accumulation in all sensory cells under control conditions (Figures 4F, F', arrows and S1G, G'). Moreover, the expression pattern was similar in Ttk69-mutant sensory organs and control sensory organs outside of the clones (Figure 4F, F'). These data show that the cis-regulatory sequence required for Ttk69-mediated down-regulation of *cycE* expression is located in the D-sequence, which does not have canonical AGGAC Ttk binding sites. Thus, Ttk69 may control *cycE* expression by binding directly to unknown binding sites located in the D-sequence or indirectly by regulating the expression of another factor that recognizes the D-sequence.

Ttk69 binds indirectly to the *cycE*-promoter

We performed a DNA-mediated Ttk pull-down assay using the Ttk69 C-terminal domain, containing the C2H2-type zinc-finger, to test whether Ttk69 binds to the *cycE*-promoter. The Ttk69 zinc-finger domain behaved as expected, since it was efficiently retained on beads coated with DNA fragments bearing canonical Ttk-binding sites (*ftz*, as well as A or C *cycE*-promoter fragments, Figure 5A, lanes 1, 3, and 5). In contrast, we observed low-level nonspecific retention when beads were coated with DNA free of Ttk binding sites (*rp49*, Figure 5A, compare lanes 1 and 2); quantification showed that binding to the *rp49* probe was reduced to 12% of that observed using the *ftz* probe. We also observed low-level nonspecific retention when the beads were coated with A or C fragments in which the Ttk binding sites were mutated (Am and Cm respectively, Figure 5A, compare lane 3 with 4 and lane 5 with 6);

binding to the Am probe was 17% of that containing A and binding to the Cm probe was 23% of that containing C. We already showed that only the D-fragment of the *cycE* promoter was necessary for the Ttk-mediated repression of *cycE* transcription. Thus, we divided the D-fragment in three (D1-D3) and assessed their role in Ttk69 binding (Figure 5B). As expected for fragments which do not harbour known Ttk-binding sites, none retained the Ttk69 zinc-finger domain (Figure 5C, top panel, compare lanes 3 to 5 to the positive *ftz*-probe (lane 1) and the negative *rp49*-probe (line 2)). These data suggest that Ttk69 represses *cycE* expression by binding to the *cycE*-promoter in association with other partners. We tested this possibility by performing DNA-mediated Ttk pull-down assays using embryonic extracts (Figure 5D). Remarkably, although endogenous Ttk69 was not retained by the D2 *cycE*-promoter fragment (Figure 5C bottom panel, lane 4), it was indeed retained on beads coated with the D1 and D3 fragments (Figure 5C, bottom panel, lanes 3 and 5). These data suggest that Ttk69 represses *cycE* expression by indirectly binding to D1 and D3 *cycE*-promoter fragments through unknown proteins.

Ttk69 downregulates *hamlet* expression

We wished to identify Ttk target genes involved in cell fate regulation in sensory organs. We focused on two candidates, *hamlet (ham)* and *sequoia (seq)* (Andrews et al., 2009; Moore et al., 2004), because the phenotype associated with *ham* and *seq* loss of function, inner to outer cell transformation, is similar to that of *ttk* gain of function. In addition, *ham* and *seq* genes are expressed in patterns that are complementary to the expression pattern of *ttk* during the bristle lineage (Figures 1A and S2, see supplementary Figure 4 in Andrews et al., 2009). We thus studied the potential epistatic interactions between these three factors.

We first studied *ttk* expression in sensory organs when *ham* and *seq* were either overexpressed or downregulated. We used a temperature conditional driver to overexpress *ham* or *seq* only when cells were already committed to differentiation to avoid potential interference with outer-to-inner cell transformations induced by *seq* or *ham*-overexpression. Under these conditions, we detected no cell fate transformations, assessed by Su(H) immunoreactivity as a marker of outer socket fate (Figure S3A-C, Su(H) panels). This analysis revealed that Ttk69 expression was unaffected when either *ham* or *seq* were overexpressed (Figure S3A-C, Ttk panels). Reciprocally, we failed to observe modifications in the number of Ttk-positive cells early during development in *ham* or *seq* mutant sensory organs (20 and 22 h APF, Figure S3D-G). We observed sensory clusters harboring four Ttk69-positive cells only late in the bristle lineage in *seq* or *ham* mutant clones (24 h APF in

12% and 34% of clusters in *ham* and *seq* mutant clones, respectively, Figure S3D-E, F and G). These data suggest that supernumerary Ttk cells in *ham* and *seq* loss of function are due to cell transformation induced by the loss of function of *seq* or *ham*, rather than direct deregulation of *ttk69* expression. Thus, we conclude that *ttk* expression is independent of Ham and Seq.

We reciprocally analyzed whether *ham* or *seq* expression are controlled by Ttk69. We thus overexpressed Ttk69 late in neurons, where it is never detected, and analyzed Seq and Ham protein accumulation. We used a similar strategy as before to overexpress Ttk69 late in development and observed no cell-fate transformation as shown by ELAV immunoreactivity (Figure 6A and B, ELAV panels). Under these conditions, Seq accumulated at the same level as in the control situation, whereas Ham immunoreactivity was strongly reduced (compare the right panels in Figure 6A and B for Seq and Ham detection; respectively). The observed effects were not due to changes in cell fate, as ELAV expression was unaltered. As such, we conclude that Ttk69 does not affect *seq* expression, whereas it downregulates *ham* expression.

Ttk69 maintained non-neural cell fate via repression of *hamlet* expression.

Our results show that Ttk69 downregulates *ham* expression. This suggests that *ham* is repressed in Ttk69 expressing cells, in particular in pIIa precursor cells and their progeny. It is thus expected that *ham* would be ectopically expressed in pIIa cells in Ttk69-mutant sensory organs. Indeed, we observed the presence of three to four Ham-positive cells in 50% of Ttk69 mutant sensory organs analyzed (sensory organs inside Ttk69 clones) at 24 h APF, whereas there were no more than two in the control sensory organs (sensory organs outside Ttk69 clones) (Figure 7A and B). However, ectopic expression of *ham* could be due to the deregulation of *ham* expression *per se* or to the cousin-cousin cell transformation already described. We assessed *ham* expression in Ttk69 mutant sensory organs at early stages to determine the mechanism behind its ectopic expression. We observed three Ham-positive cells in Ttk69 mutant sensory organs composed of four cells as early as 20 h APF, even before the completion of the bristle lineage (Figure 7A and B). These data show that the ectopic expression of *ham* in the absence of Ttk69 is an early event during the cousin-cousin cell transformation. Moreover, we occasionally observed cells positive for both Ham and Pdm1, a specific marker of pIIa descendent cells, in Ttk69 mutant sensory clusters (arrowhead in Figure 7C, C'). This signature is consistent with the cells undergoing transformation from outer to inner cells.

These data suggest that the de-repression of *ham* in pIIa cells in Ttk69 mutants drives cousin-cousin cell transformation, in which pIIa shaft cells adopt a pIIIb cell fate. We tested this possibility by studying whether the reduction of *ham* expression in Ttk69 mutant sensory organs could restore shaft identity. We performed this analysis late in bristle development, at 28 h APF, when this transformation has already taken place. Under these conditions, we observed Pdm1 positive/Su(H) negative cells, a specific sign of shaft cells, in Ttk69 mutant sensory organs in a *ham* heterozygous background (4 of 60 Ttk69 mutant sensory organs analyzed, Figure 7D-D''', arrowhead). These results show that a reduction in *ham* expression can rescue the formation of shaft cells in the absence of Ttk69. Thus, Ttk69 maintains a non-neural cell fate in pIIa daughter cells by inhibiting the adoption of the inner precursor fate via the repression of *ham* expression.

Discussion

An important goal in developmental biology is to understand the mechanisms by which cell proliferation and cell-fate acquisition are coupled during organogenesis. Here, we show that Ttk69, a member of the evolutionarily conserved BTB-ZF transcription factors, known to be involved in diverse biological processes, such as cell determination and cell proliferation, acts as a link between these two processes. We found that Ttk69 is essential for exiting the proliferative progenitor state and conferring a non-neural fate to the progeny during the formation of mechanosensory bristles. Indeed, using mainly clonal analysis, we show that ectopic cell division occurs independently of changes in cell fate. In addition, we observed that Ttk69 mutant sensory organs harbor supplementary terminal cells due to cell transformation that generates extra neural progenitor cells. This was associated with upregulation of *cycE*, required for S-phase entry, and the ectopic expression of *hamlet*, a neural determinant. As such, the BTB-ZF transcriptional factor, Ttk69, links cell proliferation and cell fate acquisition in the bristle cell lineage (Figure 8).

Ttk69 acts as a dual factor linking cell proliferation and cell fate acquisition.

Our results showed that the loss of Ttk69 leads to sensory organs harboring up to eight terminal cells. Supplementary terminal cells arose from two different mechanisms: an extra-division of socket cells and, more importantly, several rounds of extra division due to the re-specification of the presumptive shaft cell into a pIIIb precursor cell. It was previously shown that sensory organs in complete *ttk* null pupae are composed of only four neurons (Guo et al.,

1995). The fact that no ectopic cells were generated when all Ttk isoforms were absent may reflect different kinetics between cell cycle arrest and cell differentiation. *ttk* null cells rapidly acquired an arrested cell cycle and neuronal terminal fate, rather than entering a proliferative precursor state, as after Ttk69 loss of function. Thus, the specific effects of Ttk69 on the cell cycle were masked in the *ttk* null mutant. Use of the Ttk69 loss-of-function mutant made it possible to reveal intermediate cell fates, prior to the acquisition of terminal-cell identities. Moreover, the study of mutants that exclusively affect Ttk69 allowed decoupling of the acquisition of cell cycle arrest and cell fate.

The effects of Ttk69 on the core cell cycle machinery were revealed by the ectopic divisions of socket cells observed under Ttk69 loss of function conditions. These cells are already committed to acquire a terminal identity, indicating that such ectopic divisions are not associated with changes in cell fate. This shows that Ttk69 impedes cell cycle progression *per se*. Accordingly, we show that the control of cell-cycle progression by Ttk69 involves transcriptional downregulation of *cycE* expression. Such negative control of *cycE* expression by Ttk69 appears to be a general effect, as it has also been observed in proliferating glia cells (Badenhorst, 2001). Moreover, it has also been shown that Ttk69 represses the expression of *string*, which encodes the phosphatase (Cdc25) essential for G2/M transition in the imaginal eye disc (Baonza et al., 2002). This suggests that Ttk69 represses cell-cycle progression at different phases of the cell cycle. Thus, the induction of ectopic cell divisions in the absence of Ttk69 is probably due to the multiple effects of Ttk69 on cell-cycle progression. The diverse targets of Ttk69 in the cell cycle machinery could explain the involvement of this factor in the transition between different modes of the cell cycle (Jordan et al., 2006; Sun et al., 2008). In sensory organs, pIIa terminal cells underwent endocycles that require the fine-tuned control of *cycE* expression. Indeed, we have already shown that endocycles are abolished in *cycE* null mutants, occur at very low CycE levels, and become mitotic cycles at high CycE levels (Sallé et al., 2012; Simon et al., 2009). We show here that Ttk69 is involved in a mechanism that limits CycE levels. Thus, Ttk69 is probably involved in the transition from mitotic cell cycles to endocycles in pIIa terminal cells. Similar transitions between two cycling states associated with two different levels of Ttk69 have been observed in ovary epithelial follicular cells during the transition between endocycles to gene amplification (Jordan et al., 2006; Sun et al., 2008). We propose that Ttk69 contributes to the dampening of *cycE* levels, allowing cells to transit throughout different modes of the cell cycle.

In addition to cell proliferation, both pIIa daughter cells were differentially affected under Ttk69 mutant conditions, at the level of terminal differentiation for socket cells and determination for shaft cells. For socket cells, although sensory organs of adult Ttk69 mutants contain socket cuticular structures, auto-amplification of Su(H) expression is impaired, leading to misshapen sockets (Barolo et al., 2000). For shaft cells, presumptive shaft cells are re-specified and acquire a neural progenitor identity due to the mis-expression of *ham*. Ham is normally expressed in pIIIb precursor cells and its overexpression induces the formation of sensory organs bearing supernumerary cells expressing both ELAV and Pros, such as in pIIIb cells (see Figure 4 in Moore et al., 2004). In addition, *ham* loss of function induces the conversion of terminal inner cells into outer cells, suggesting that Ham is essential to acquire the neural precursor fate (Moore et al., 2004). Moreover, we observed that a reduction of *ham* levels in *ttk69* mutant clones decreased shaft re-specification, in agreement with the fact that Ham is an essential regulator of neural precursor fate. Finally, we show that Ttk69 repressed *ham* expression. Overall, these data suggest that re-specification of shaft cells is due to the ectopic expression of *ham* as a consequence of the loss of function of Ttk69. *ham* was also mis-expressed in socket cells, but did not lead to cell transformation. This apparent contradiction may be related with the differential activation of the N-pathway between these two sister cells. Indeed, Ttk69 loss of function induces a cell fate change in shaft cells, a Noff cell. In contrast, Ttk69 loss of function in socket cells, in which the N-pathway is activated as soon as the cells are formed (Remaud et al., 2008), impaired only their late differentiation. These results suggest that early activation of the N-pathway prevents cell fate transformation.

We conclude that Ttk69 is required in terminal cells to represses the neural precursor state by inhibiting both proliferative capacity, by repressing *cycE* expression, and neural fate, by repressing *ham*. This shows that Ttk69 is a central actor in the coordination between cell cycle arrest and cell fate acquisition.

Tt69 regulates its target genes in several ways.

In this study, we identified three Ttk69 target genes, *cycE*, *ham*, and *Su(H)*. *Su(H)* is positively regulated by Ttk69, as revealed by its down-regulation in socket cells in the Ttk69 mutant context. The action of Ttk69 on *Su(H)* enhancer may occur in two different ways. Either Ttk69 acts directly as a transcriptional activator or it represses the expression of an unknown factor, as Ttk69 has always been described as a transcriptional repressor. The time required to express this putative relay factor is consistent with the observation that Ttk69 loss

of function affected only late socket cell differentiation. Furthermore, we showed that such Ttk69-mediated regulation occurs through the *Su(H)* 3'end auto-regulatory enhancer, ASE5. It is interesting to note that, the long-lasting high-level of *Su(H)* expression mediated by the auto-regulatory ASE5 loop does not requires N-pathway signaling (Liu and Posakony, 2014). As such, once again Ttk69 loss of function affected Notch-independent processes. Further experiments are required to elucidate how Ttk69 activates the auto-amplification of *Su(H)* expression.

In contrast to the downregulation of *Su(H)*, we observed upregulation of *cycE* in the absence of Ttk69, in accordance with the canonical Ttk function as a transcriptional repressor. Surprisingly, Ttk69-mediated *cycE* down-regulation was driven through a promoter domain (fragment D) that is devoid of the canonical AGGAC Ttk69 binding sites (Brown et al., 1991). Accordingly, we showed that the Ttk69 zinc-finger domain does not bind the D fragment, whereas the native Ttk69 protein, present in a late embryonic extract, does. There are two non-exclusive explanations for this observation. Either an uncharacterized Ttk69 domain outside the zinc-finger domain binds directly to the D fragment through a non-canonical binding site or Ttk69 binds indirectly to the *cycE* promoter via an interaction with *trans*-acting factors. The first explanation is formally possible, but no DNA binding domain has been described in the N-terminal portion of the Ttk69 protein. Nevertheless, it is well known that Ttk69 may bind to other non-canonical binding sites. This is the case for the GTCCTG and TTATCCG sequences in *eve* and *ftz* promoters respectively (Harrison and Travers, 1990; Read and Manley, 1992). However, we observed that Ttk69 continued to downregulate cycE expression in the absence of these non-canonical sites, making this explanation unlikely. In contrast, several lines of evidence support the second explanation. It is known that the activity of Ttk69 can be influenced by the presence of other DNA-binding factors. Thus, the repressive action of Ttk69 depends on interactions with MEP1 and Mi2 proteins, which recruit the ATP-dependent chromatin-remodeling complex (NuRD) (Reddy et al., 2010). Moreover, it has been shown that, although Ttk could bind directly to *eve* promoter repressing *eve* expression (see above), Ttk69 repress *eve* expression independently of their direct binding to DNA, by interacting with GAGA factors through its BTB/POZ domain. When bound to DNA, GAGA zinc-finger factors (Trithorax-like, Trl) activate the transcriptional machinery, but this transcription is inhibited when it is complexed with Ttk69 (Pagans et al., 2004). RNAi-mediated loss of function of the *MEP1, Mi2*, and *Trl* genes did not affect cell number or cell fates, even when these loss-of-function mutations were analyzed

in a sensitized *ttk69* heterozygous background (Figure S3). Despite these results, we favor a model in which another factor is required for Ttk69 to bind the D fragment of the *cycE* promoter. Furthermore, we did not find Ttk binding close to the *cycE* promoter using genome-wide Ttk binding profiles from 0 to 12-h old embryos, published by the modENCODE project. Moreover, *cycE* up-regulation was not observed in genome-wide expression experiments performed in S2 cells treated with dsRNA directed against Ttk69 (Reddy et al., 2010). These data suggest that Ttk69 does not regulate *cycE* expression during early embryonic stages. Thus, Ttk-mediated downregulation of *cycE* expression late in development probably requires cell specific *trans*-acting factors.

The involvement of *trans*-acting factors would explain the diversity of the Ttk response of particular cells at specific developmental stages. Such diversity mediated by trans-acting factors allows Ttk to regulate the expression of a broad spectrum of genes in bristle sensory cells in response to N-pathway activation, (Figure 8). This is true not only for genes related to cell proliferation, such as *cycE*, but also those controlling cell fate, such as *ham* and *Su(H)*. Ttk represses *ham* in pIIa sublineage cells and activates the *Su(H)* autoregulatory loop in socket cells. *cycE* and *ham* regulation occur earlier in this lineage and likely involves the binding of Ttk69 to gene promoters as we have shown for *cycE*. In contrast, Su(H) regulation takes place late in the lineage, implying the probable repression of intermediary relay factors. *Trans*-acting factors would allow cell-specific responses to Ttk69, whereas intermediary relay factors would allow diversification over time. Thus, the mechanism of action of Ttk69 increases the spatial and temporal diversity of the N-pathway cell response.

Materials and methods

Fly strains

Somatic clones were obtained using the FLP/FRT recombination system (Xu and Rubin, 1993). The *y, w; FRT82B ttk^{1e11}/CyO*^SM5 line (41754 Bloomington) was crossed with the *y, w, Ubx-FLP; FRT82B ubi-nls::GFP* line (gift of J. Knoblich) to generate *ttk69*-null somatic clones. Somatic *ham* and *seq* clones were generated using the *y, w; FRT40A ham^{1}/CyO*^SM5 (gift from YN. Jan) crossed with *y, w, Ubx-FLP; FRT40A ubi-nls::GFP and y, w; FRT42D seq^{A41}/CyO*^SM5 *(gift from H. Bellen)* crossed to *y, w; UbxFLP, FRT42A ubi-nls::GFP*, respectively.

Analysis of the Ttk69 loss of function on a *ham* heterozygous background was obtained using a *y, w; FRT40A ham^{1}; FRT82B ttk^{1e1}/CyO*^SM5 crossed with *y, w, UbxFLP; FRT82B ubi-nls::GFP*.

Analysis of the Ttk69 loss of function on a *cycE* heterozygous background was obtained using a *y, w; cycE^{AR95}; FRT82B ttk^{1e11}/CyO^SM5* crossed with *y, w, Ubx-FLP; FRT82B ubi-nls::GFP*.

To study Su(H) auto-amplification under Ttk69 loss-of-function conditions, the line y, w; *ASE5-GFP; FRT82B ttk^{1e11}/CyO^SM5* was crossed with *y, w, Ubx-FLP; FRT82B ubi-nls::GFP*.

To analyze the cycE promoter, the following *cycE* transcriptional reporter lines were used: (*y, w; cycE-16.4-lacZ),* (*y, w; cycE-4.6-lacZ),* (*y, w; cycE-ACm-lacZ),* (*y, w; cycE-ΔAC-lacZ),* (*y, w; cycE-ΔB-lacZ) and* (*y, w; cycE-ΔD-lacZ).*

These cycE transcriptional reporters were analyzed under Ttk69 loss-of-function conditions in pupae at 28 h APF in lines obtained after crossing *y, w, Ubx-FLP; FRT 82B, nls-GFP / TM6 Tb* with the following lines (*16.4WT-lacZ;* FRT82B *ttk^{1e11}*/ TM6 Tb), (*4,6WT-lacZ;* FRT82B *ttk^{1e11}*/ TM6 Tb), (ΔCm-*lacZ;* FRT82B *ttk^{1e11}*/ TM6 Tb), (*ΔD-lacZ;* FRT82B *ttk^{1e11}*/ TM6 Tb).

The GAL4/UAS expression system (Brand and Perrimon, 1993) was used to express the following UAS-constructions in the mechanosensory bristle cell lineage using, as a GAL4 driver, the line *neuralized^{p72}-Gal4 (neur^{p72})* (Bellaïche et al., 2001), *UAS-histone H2B::YFP (UAS-H2B::YFP)* (Bellaïche et al., 2001), *UAS-tramtrack69 (UAS-ttk69)* (Badenhorst, 2001),

UAS-hamlet (UAS-*ham*), *UAS-sequoia* (UAS-*seq*) (gift from H. Bellen), UAS-$trl^{RNA\text{-}valium}$ (Bloomington, 40940 and 41582), *UAS-mep1* (Bloomington, 35399; VDRC, 24534) and *UAS-mi-2* (VDRC, 100517). We use the temperature conditional line *UAS-H2B::YFP;* $neur^{p72}$*,* $tub\text{-}GAL80^{ts}$ to overexpress these constructs late during sensory organ formation. Fly crosses were carried out at 18°C and pupae were transferred to 30°C at 21 h APF. Pupae were fixed and dissected 7 h later.

Genotypes used in each figures are recapitulated in Supplementary Table-1.

Immunohistology

Pupal nota were dissected at 17-32 h APF and processed as previously described (Gho et al., 1996). Primary antibodies were: mouse anti-Cut (DSHB, #2B10, 1:500); rabbit anti-β-Galactosidase (Cappel; #55976; 1:500); rabbit anti-GFP (Santa-Cruz Biotechnology, #sc-8334; 1:500); mouse anti-GFP (Roche, N° 11 814 460 001, 1:500), rabbit anti-Pdm1 (gift from T. Préat; École Supérieure de Physique et de Chimie Industrielles, Paris, France; 1:200), rabbit anti-Ttk69 (gift from A. Travers, Medical Research Council, Cambridge, United Kingdom; 1:500), rabbit anti-Ham (gift from YN. Jan, Howard Hughes Medical Institute, San Francisco, USA; 1:500), rabbit anti-Seq (gift from H. Bellen, Baylor College of Medicine, Houston, USA; 1:500); rat anti-ELAV (DSHB, #7E8A10, 1:10); mouse anti-ELAV (DSHB, #9F8A9; 1:100); mouse anti-Pros (1:5, gift from C. Doe, Institute of Neuroscience, Eugene, USA), rat anti-Su(H) (gift from F Schweisguth, Institut Pasteur, Paris, France 1:500), and rabbit anti-phospho-Histone H3 (Upstate, 06-510, 1:10000). Alexa 488-conjugated secondary anti-mouse (#A11029), anti-rat (#A11006), anti-rabbit (#A11034), Alexa 568-conjugated secondary anti-mouse (#A11031), anti-rat (#A11077), and anti-rabbit (#A11011) were purchased from Molecular Probes and used at 1:1000. Cy5-conjugated antibodies anti-mouse (#715-175-151), anti-rat (#712-175-153), or anti-rabbit (#711-175-152) were purchased from Jackson Immunoresearch and were used at 1:2000. DNA fragmentation was assayed by TdT-mediated dUTP nick end labelling and performed as previously described (Fichelson and Gho, 2003) (TUNEL kit, Roche Molecular Biochemical). Images were processed with NIH-Image and Photoshop software.

Time lapse microscopy

We performed live imaging of sensory organs in *neur-H2B::GFP; FRT82B* ttk^{1e11} pupae following protocols described previously (Sallé et al., 2012; Simon et al., 2009). The

construction *neur-H2B::GFP* (line 22A4, gift of F. Schweisguth) allows the following of sensory organ cells throughout the progression of the bristle lineage. White pupae were collected and aged until 20 h APF at 25°C in a humid chamber before dissection and mounting for imaging. Live imaging data were collected using a spinning disk coupled to an Olympus BX-41 microscope (Roper Scientific, 40X, NA 0.75 objective, CoolSnapHQ2 camera). The temperature of the recording chamber was carefully controlled (±0.1°C) using a homemade Peltier device temperature controller fixed to the microscope stage. Systems were driven by Metamorph software (Universal Imaging). Z-stacks of images were acquired every 3 min and assembled using ImageJ software (NIH). At the end of the movies, pupae were dissected and immunostaining were carried out as described previously. Imaged cells were unambiguously identified by their relative position, nuclear size, and order of birth.

Tramtrack69 pull down.

Experiments were performed either using a batch of *E. coli*-expressed Ttk69::ZF or 20 h old *white drosophila* embryo protein extracts. Ttk69::ZF was expressed from BL21 (DE3) bacteria transformed with a pET15 vector in which the C-terminal fragment (318–641) of Ttk69 protein, containing zinc fingers, was cloned in-frame with a histidine tag (gift from A. Travers). Non-denatured *E. coli* extracts were prepared after a 2 h induction in 0.1mM IPTG and embryo extracts were obtained as described by Wordarz (Wodarz, 2008), 1 mg devitellinized embryos was always extracted in 5 µl lysis buffer to calibrate extraction). DNA templates were generated by PCR using 5' biotinylated primers. As controls, a Ftz template was obtained using 5'GGGAGTTGCGCACTTGCTTG and 5'GTGCACGCAACGCTGGTGAG primers, which correspond to the portion of the *fushi-tarazu (ftz) promotor* bearing the canonical AGGAC Ttk69 binding sites and a *RP49* template devoid of this sequence was obtained using 5' TGTACTTGGCATCCGCGAG and 5' CACCAGCACTTCTCCAACAC. Two *cycE* templates were obtained using 5' GCAAGATTATGAATATCTAT and 5' GTGTGCGCGCATGCGCAACG and 5' GTTGGATTAACCCTTTCTGG 5' AGGATTTAAGTCTCAACTC to cover fragments A and C, respectively, which correspond to the proximal part of the promoter bearing the canonical Ttk69 AGGAC. Am and Cm *cycE* mutated promoters, in which all canonical AGGAC sequences were replaced by a ACTGC sequences, were obtained using the same primers as for fragments A and C of the *cycE* promoter. The three *cycE* templates corresponding to the D fragment are obtained using primers

5'GCTGCCTGCTTGGAGTTGAGAC and 5'GGAAGGTCCAAGACGCATGAC for the D1 fragment, 5' GTCATGCGTCTTGGACCTTCC, 5'TGCCCAATATCTGCACATAA, and 5'TTATGTGCAGATATTGGGCA for the D2 fragment, and 5'TTATGTGCAGATATTGGGCA and 5' CTCGAGCTGCCAGCGGCTGC for the D3 fragment. Biotinylated DNA was coupled to streptavidin-coated magnetic beads (M280, Dynal Biotechnology) with 0.1 mg beads per 200 ng DNA, overnight at 4°C. The beads were washed three times in B&W buffer (as recommended by the supplier) and streptavidin-immobilized DNA saturated for 1 h in PBS-20% horse serum before incubation for 1 h with the protein extract in PBS-Triton (0.15%). Protein extracts and beads were separated according to the manufacturer's instructions and washed four times with 100 mM NaCl/25 mM NaH_2PO_4. Each fraction was then processed for electrophoreses on SDS polyacrylamide gels. Ttk69::ZF was revealed using mouse anti-Penta-Histidine (1:1000; Qiagen; 34660), whereas Ttk69 protein from embryo extracts was revealed using rabbit anti-Ttk69 (1:4000 gift from A. Travers). Specificity of the Ttk69 antibody was tested by analyzing the immuno-detection of protein extracts from pools of ten 20 h old ttk^{le11}/TM6 and w^{1118} embryos. Anti-β tubulin staining (1:10000, Amersham) was used as a loading control. Revelation was performed using horseradish peroxidase coupled to anti-mouse or anti-rabbit (1:10000, Promega) antibodies coupled to the Super Signal Western blotting detection system (Pierce) according to the manufacturer's instructions.

Acknowledgements

We specially thank YN. Jan, J. Knoblich, H. Bellen, H. Richardson and A. Travers for antibodies. The fly community for fly strains. Heather McLean and Jérôme Lacoste for critical reading.

Funding

Funding was provided by the Centre National de la Recherche Scientifique and the Sorbonne Université. Anne Ramat was financed by grants from the Ministère de l'Education Nationale et de la Recherche and the Association pour la Recherche sur le Cancer, France. The funders had no role in study design, data collection and interpretation, or the decision to submit the work for publication.

Author contributions

Françoise Simon, Anne Ramat, Angélique Burg, Agnès Audibert performed the experiments and carried out data analysis. Agnès Audibert, Sophie Louvet-Vallée, Michel Gho conceptualize, designed experiments and carried out data analysis. Agnès Audibert, Sophie Louvet-Vallée, Michel Gho prepared and edited the manuscript.

References

Andrews, H. K., Giagtzoglou, N., Yamamoto, S., Schulze, K. L. and Bellen, H. J. (2009). Sequoia regulates cell fate decisions in the external sensory organs of adult Drosophila. *EMBO Rep*. **10**, 636–641.

Araujo, S. J., Cela, C. and Llimargas, M. (2007). Tramtrack regulates different morphogenetic events during Drosophila tracheal development. *Development* **134**, 3665–3676.

Audibert, A., Simon, F. and Gho, M. (2005). Cell cycle diversity involves differential regulation of Cyclin E activity in the Drosophila bristle cell lineage. *Dev. Camb. Engl.* **132**, 2287–2297.

Badenhorst, P. (2001). Tramtrack controls glial number and identity in the Drosophila embryonic CNS. *Development* **128**, 4093–4101.

Baonza, A., Murawsky, C. M., Travers, A. A. and Freeman, M. (2002). Pointed and Tramtrack69 establish an EGFR-dependent transcriptional switch to regulate mitosis. *Nat. Cell Biol*. **4**, 976–980.

Barolo, S., Walker, R. G., Polyanovsky, A. D., Freschi, G., Keil, T. and Posakony, J. W. (2000). A Notch-Independent Activity of Suppressor of Hairless Is Required for Normal Mechanoreceptor Physiology. *Cell* **103**, 957–970.

Bellaïche, Y., Gho, M., Kaltschmidt, J. A., Brand, A. H. and Schweisguth, F. (2001). Frizzled regulates localization of cell-fate determinants and mitotic spindle rotation during asymmetric cell division. *Nat. Cell Biol*. **3**, 50–57.

Bonchuk, A., Denisov, S., Georgiev, P. and Maksimenko, O. (2011). Drosophila BTB/POZ Domains of "ttk Group" Can Form Multimers and Selectively Interact with Each Other. *J. Mol. Biol*. **412**, 423–436.

Brand, A. H. and Perrimon, N. (1993). Targeted gene expression as a means of altering cell fates and generating dominant phenotypes. *Development* **118**, 401–15.

Brown, J. L., Sonoda, S., Ueda, H., Scott, M. P. and Wu, C. (1991). Repression of the Drosophila fushi tarazu (ftz) segmentation gene. *EMBO J*. **10**, 665–674.

Chaharbakhshi, E. and Jemc, J. C. (2016). Broad-complex, tramtrack, and bric-à-brac (BTB) proteins: Critical regulators of development. *Genes. N. Y. N 2000* **54**, 505–518.

Fichelson, P. and Gho, M. (2003). The glial cell undergoes apoptosis in the microchaete lineage of Drosophila. *Dev. Camb. Engl*. **130**, 123–133.

Fichelson, P., Audibert, A., Simon, F. and Gho, M. (2005). Cell cycle and cell-fate determination in Drosophila neural cell lineages. *Trends Genet. TIG* **21**, 413–420.

Gaber, Z. B., Butler, S. J. and Novitch, B. G. (2013). PLZF regulates fibroblast growth factor responsiveness and maintenance of neural progenitors. *PLoS Biol*. **11**, e1001676.

Gho, M., Lecourtois, M., Géraud, G., Posakony, J. W. and Schweisguth, F. (1996). Subcellular localization of Suppressor of Hairless in Drosophila sense organ cells during Notch signalling. *Dev. Camb. Engl*. **122**, 1673–1682.

Gho, M., Bellaïche, Y. and Schweisguth, F. (1999). Revisiting the Drosophila microchaete lineage: a novel intrinsically asymmetric cell division generates a glial cell. *Dev. Camb. Engl*. **126**, 3573–3584.

Giesen, K., Hummel, T., Stollewerk, A., Harrison, S., Travers, A. and Klambt, C. (1997). Glial development in the Drosophila CNS requires concomitant activation of glial and repression of neuronal differentiation genes. *Development* **124**, 2307–2316.

Guo, M., Bier, E., Jan, L. Y. and Jan, Y. N. (1995). tramtrack acts downstream of numb to

specify distinct daughter cell fates during asymmetric cell divisions in the Drosophila PNS. *Neuron* **14**, 913–925.
Guo, M., Jan, L. Y. and Jan, Y. N. (1996). Control of daughter cell fates during asymmetric division: interaction of Numb and Notch. *Neuron* **17**, 27–41.
Harrison, S. D. and Travers, A. A. (1988). Identification of the binding sites for potential regulatory proteins in the upstream enhancer element of the Drosophila fushi tarazu gene. *Nucleic Acids Res*. **16**, 11403–11416.
Harrison, S. D. and Travers, A. A. (1990). The tramtrack gene encodes a Drosophila finger protein that interacts with the ftz transcriptional regulatory region and shows a novel embryonic expression pattern. *EMBO J*. **9**, 207–216.
Hartenstein, V. and Posakony, J. W. (1989). Development of adult sensilla on the wing and notum of Drosophila melanogaster. *Dev*. *Camb*. *Engl*. **107**, 389–405.
Jin, Y., Nenseth, H. Z. and Saatcioglu, F. (2017). Role of PLZF as a tumor suppressor in prostate cancer. *Oncotarget* **8**, 71317.
Jones, L., Richardson, H. and Saint, R. (2000). Tissue-specific regulation of cyclin E transcription during Drosophila melanogaster embryogenesis. *Development* **127**, 4619–4630.
Jordan, K. C., Schaeffer, V., Fischer, K. A., Gray, E. E. and Ruohola-Baker, H. (2006). Notch signaling through tramtrack bypasses the mitosis promoting activity of the JNK pathway in the mitotic-to-endocycle transition of Drosophila follicle cells. *BMC Dev*. *Biol*. **6**, 16.
Karim, F. D., Guild, G. M. and Thummel, C. S. (1993). The Drosophila Broad-Complex plays a key role in controlling ecdysone-regulated gene expression at the onset of metamorphosis. *Development* **118**, 977–988.
Kelly, K. F. and Daniel, J. M. (2006). POZ for effect – POZ-ZF transcription factors in cancer and development. *Trends Cell Biol*. **16**, 578–587.
Lai, Z. C. and Li, Y. (1999). Tramtrack69 is positively and autonomously required for Drosophila photoreceptor development. *Genetics* **152**, 299–305.
Liu, F. and Posakony, J. W. (2014). An Enhancer Composed of Interlocking Submodules Controls Transcriptional Autoregulation of Suppressor of Hairless. *Dev*. *Cell* **29**, 88–101.
Liu, T. M., Lee, E. H., Lim, B. and Shyh-Chang, N. (2016). Concise Review: Balancing Stem Cell Self-Renewal and Differentiation with PLZF. *Stem Cells Dayt*. *Ohio* **34**, 277–287.
McConnell, M. J., Chevallier, N., Berkofsky-Fessler, W., Giltnane, J. M., Malani, R. B., Staudt, L. M. and Licht, J. D. (2003). Growth Suppression by Acute Promyelocytic Leukemia-Associated Protein PLZF Is Mediated by Repression of c-myc Expression. *Mol*. *Cell*. *Biol*. **23**, 9375–9388.
Moore, A. W., Jan, L. Y. and Jan, Y. N. (2002). hamlet, a binary genetic switch between single- and multiple- dendrite neuron morphology. *Science* **297**, 1355–1358.
Moore, A. W., Roegiers, F., Jan, L. Y. and Jan, Y.-N. (2004). Conversion of neurons and glia to external-cell fates in the external sensory organs of Drosophila hamlet mutants by a cousin-cousin cell-type respecification. *Genes Dev*. **18**, 623–628.
Pagans, S., Piñeyro, D., Kosoy, A., Bernués, J. and Azorín, F. (2004). Repression by TTK69 of GAGA-mediated Activation Occurs in the Absence of TTK69 Binding to DNA and Solely Requires the Contribution of the POZ/BTB Domain of TTK69. *J*. *Biol*. *Chem*. **279**, 9725–9732.
Ramat, A., Audibert, A., Louvet-Vallée, S., Simon, F., Fichelson, P. and Gho, M. (2016). Escargot and Scratch regulate neural commitment by antagonizing Notch activity in Drosophila sensory organs. *Dev*. *Camb*. *Engl*. **143**, 3024–3034.
Read, D. and Manley, J. L. (1992). Alternatively spliced transcripts of the Drosophila tramtrack gene encode zinc finger proteins with distinct DNA binding specificities. *EMBO J*. **11**, 1035–1044.

Reddy, B. A., Bajpe, P. K., Bassett, A., Moshkin, Y. M., Kozhevnikova, E., Bezstarosti, K., Demmers, J. A., Travers, A. A. and Verrijzer, C. P. (2010). Drosophila transcription factor Tramtrack69 binds MEP1 to recruit the chromatin remodeler NuRD. *Mol. Cell. Biol.* **30**, 5234–5244.

Remaud, S., Audibert, A. and Gho, M. (2008). S-phase favours notch cell responsiveness in the Drosophila bristle lineage. *PloS One* **3**, e3646.

Sahut-Barnola, I., Godt, D., Laski, F. A. and Couderc, J. L. (1995). Drosophila ovary morphogenesis: analysis of terminal filament formation and identification of a gene required for this process. *Dev. Biol.* **170**, 127–135.

Sallé, J., Campbell, S. D., Gho, M. and Audibert, A. (2012). CycA is involved in the control of endoreplication dynamics in the Drosophila bristle lineage. *Dev. Camb. Engl.* **139**, 547–557.

Siggs, O. M. and Beutler, B. (2012). The BTB-ZF transcription factors. *Cell Cycle Georget. Tex* **11**, 3358–3369.

Simon, F., Fichelson, P., Gho, M. and Audibert, A. (2009). Notch and Prospero repress proliferation following cyclin E overexpression in the Drosophila bristle lineage. *PLoS Genet.* **5**, e1000594.

Sobieszczuk, D. F., Poliakov, A., Xu, Q. and Wilkinson, D. G. (2010). A feedback loop mediated by degradation of an inhibitor is required to initiate neuronal differentiation. *Genes Dev.* **24**, 206–218.

Sun, J., Smith, L., Armento, A. and Deng, W.-M. (2008). Regulation of the endocycle/gene amplification switch by Notch and ecdysone signaling. *J. Cell Biol.* **182**, 885–896.

Wang, C., Guo, X., Dou, K., Chen, H. and Xi, R. (2015). Ttk69 acts as a master repressor of enteroendocrine cell specification in Drosophila intestinal stem cell lineages. *Dev. Camb. Engl.* **142**, 3321–3331.

Wodarz, A. (2008). Extraction and immunoblotting of proteins from embryos. *Methods Mol. Biol. Clifton NJ* **420**, 335–345.

Xu, T. and Rubin, G. M. (1993). Analysis of genetic mosaics in developing and adult Drosophila tissues. *Development* **117**, 1223–37.

Zollman, S., Godt, D., Prive, G. G., Couderc, J. L. and Laski, F. A. (1994). The BTB domain, found primarily in zinc finger proteins, defines an evolutionarily conserved family that includes several developmentally regulated genes in Drosophila. *Proc. Natl. Acad. Sci.* **91**, 10717–10721.

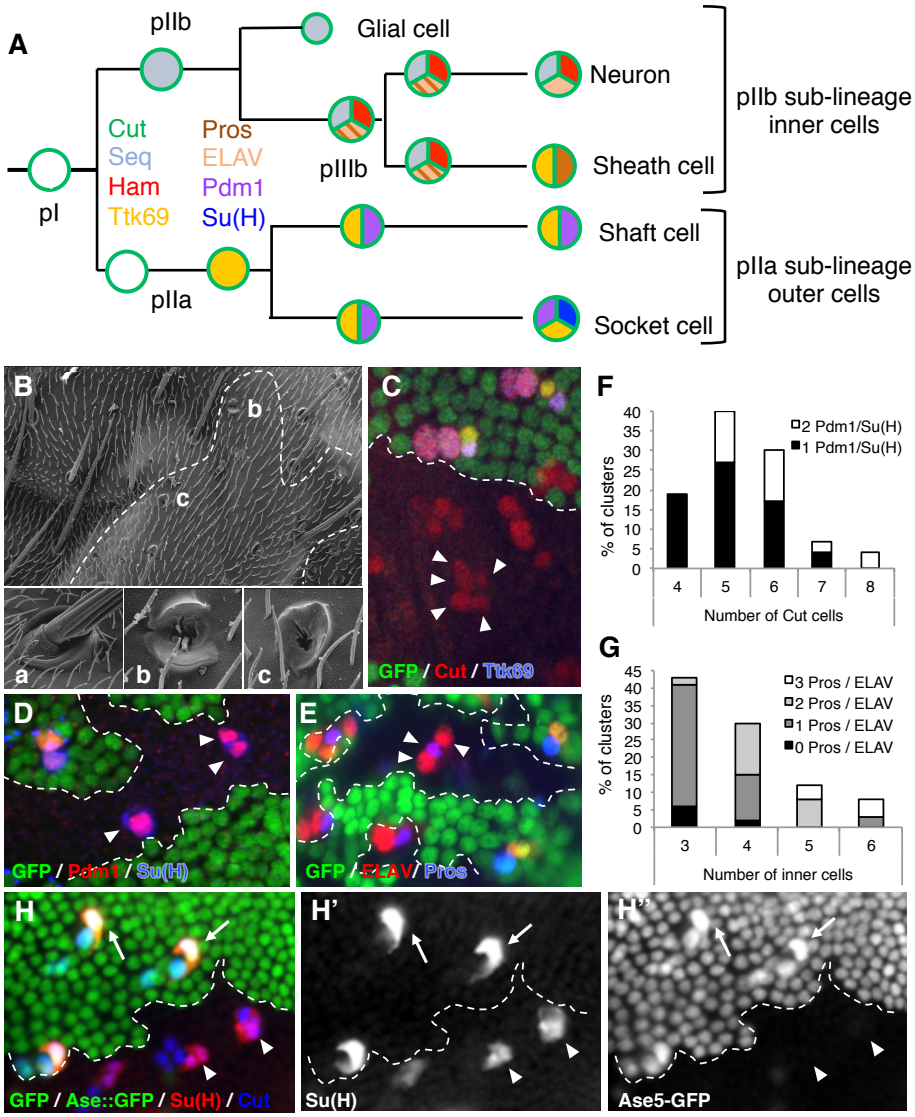

Figure 1. Ttk69 loss of function leads to extra-terminal cells in sensory organs. (A) Scheme of the wild type bristle lineage and cell markers used. Cells are represented by circles with the expression of nine molecular markers indicated in color. Markers: Cut in green; Prospero (Pros) in brown; ELAV in beige; Tramtrack69 (Ttk69) in orange; Hamlet (Ham) in red; Sequoia (Seq) in light blue; Pdm1 in purple; and Suppressor of Hairless (Su(H)) in dark blue. (B) Scanning electron micrograph showing Ttk69 mutant sensory organs at the external level. The Ttk69 clone is outlined by a white dashed line. Panels a-c: control socket (a) and Ttk69 mutant sensory organs (b and c). (C-E) Ttk69 mutant sensory organs at the cellular level. Ttk69 clones were detected by the absence of GFP. The white dashed line shows the clonal border. Pupae were at 28 h APF. (C) Ttk69 mutant sensory organs were composed of more than four cells (arrowheads). Sensory cells were identified by Cut (red) and Ttk69 (blue) immunoreactivity. (D) Outer cells acquired a socket fate: specific outer-cell marker Pdm1 in red, socket marker Su(H) in blue. Note that all outer cells marked by Pdm1 were also Su(H) positive in Ttk69 mutant sensory organs (inside Ttk69 clones, arrowheads). (E) More than two inner cells (arrowheads) are present in Ttk69 mutant sensory organs. Inner cells are revealed by ELAV (red) and Pros (blue) immunoreactivity. (F, G) Number of sensory cells of each type in Ttk69 mutant sensory organs. (F) Histogram showing the percentage of sensory organs harboring four to eight sensory cells. The percentage of sensory organs with one (black bars) or two (white bars) socket cells is indicated. (G) Histogram showing the percentage of sensory organs harboring three to six pIIb terminal cells. The percentage of clusters with zero (black bars), one (dark grey bars), two (light grey bars), or three (white bars) inner cells positive for both Pros and ELAV immunoreactivity (Pros/ELAV) is indicated. (H-H") Auto-amplification of Su(H) was impaired in Ttk69 mutant sensory organs. Su(H) immunoreactivity (H' and red in H). Su(H) auto-amplification was revealed by GFP accumulation using a ASE5::GFP reporter (H'' and green in H). Socket cells strongly accumulate GFP in control sensory organs outside Ttk69 clones (arrows), whereas they were devoid of GFP in Ttk69 mutant sensory organs (located inside Ttk69 clones, arrowheads).

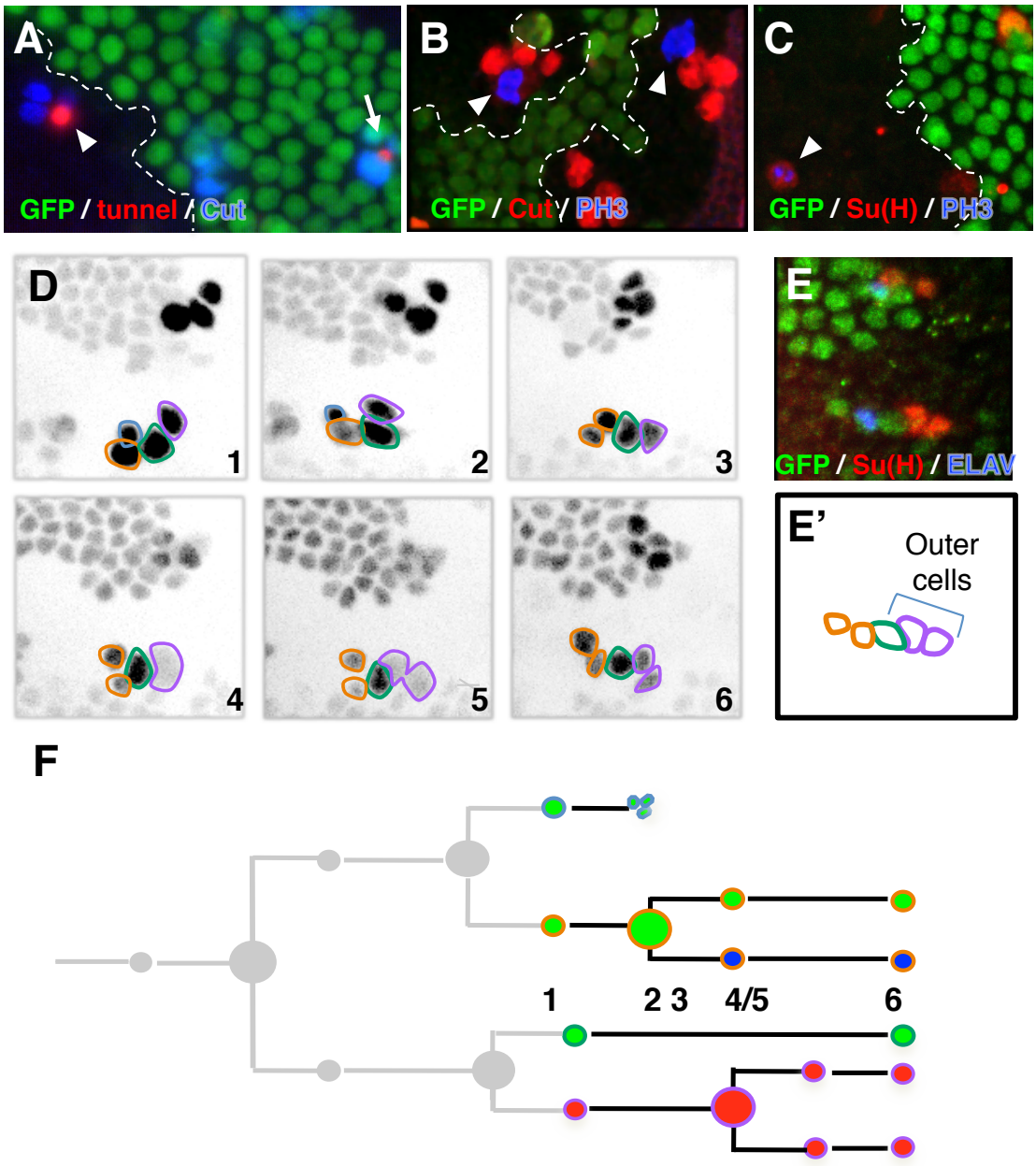

Figure 2. Extra mitoses in Ttk69 mutant socket cells. (A-C) Ttk69 clones detected by the absence of GFP (green). The white line shows the clonal border. Pupae were from between 28 and 36 h APF. (A) Sensory cells were identified by Cut immunoreactivity (blue). Apoptotic cells were detected by TUNEL staining (red). Note that cell death occurs at the same time in the mutant (arrowhead) and control (arrow) sensory organs. (B) Extra mitoses (arrowheads) revealed by PH3 immunoreactivity (blue) in Ttk69 mutant sensory organs composed of four cells (red). (C) Cell divisions in full-determined socket cells. Note that PH3 (blue) and Su(H) (red) immunoreactivity is detected in the same cell (arrowhead). (D, E) Combined 4D live imaging and lineage analysis showing an extra division of socket cells. A Ttk69 clone was identified by the lack of GFP expression in epithelial cells and sensory organs inside the clones were imaged. (D) Representative frames (1-6), depicted in inverted fluorescence, from a time-lapse recording of one Ttk69 mutant sensory organ at 19 h APF. The glial cell is outlined in blue, pIIb and its progeny in orange, the shaft cell in green, and the socket cell and its daughter in purple. Note the division of socket cells in frames 4 and 5. Note also the apoptosis of the glial cell between frames 2 and 3. (E, E') Immunostaining and schematic representation of the same cluster after the time-lapse recording shown in D. Non-clonal epithelial and sensory cells are visualized by GFP expression (green). Neurons and socket cells are identified by anti-ELAV (blue) and anti-Su(H) (red) immunoreactivity, respectively. Note that two socket cells were identified. (F) Schematic view of the lineage shown in D. Cells are encircled using the same color code as in D and filled with the same color as in E.

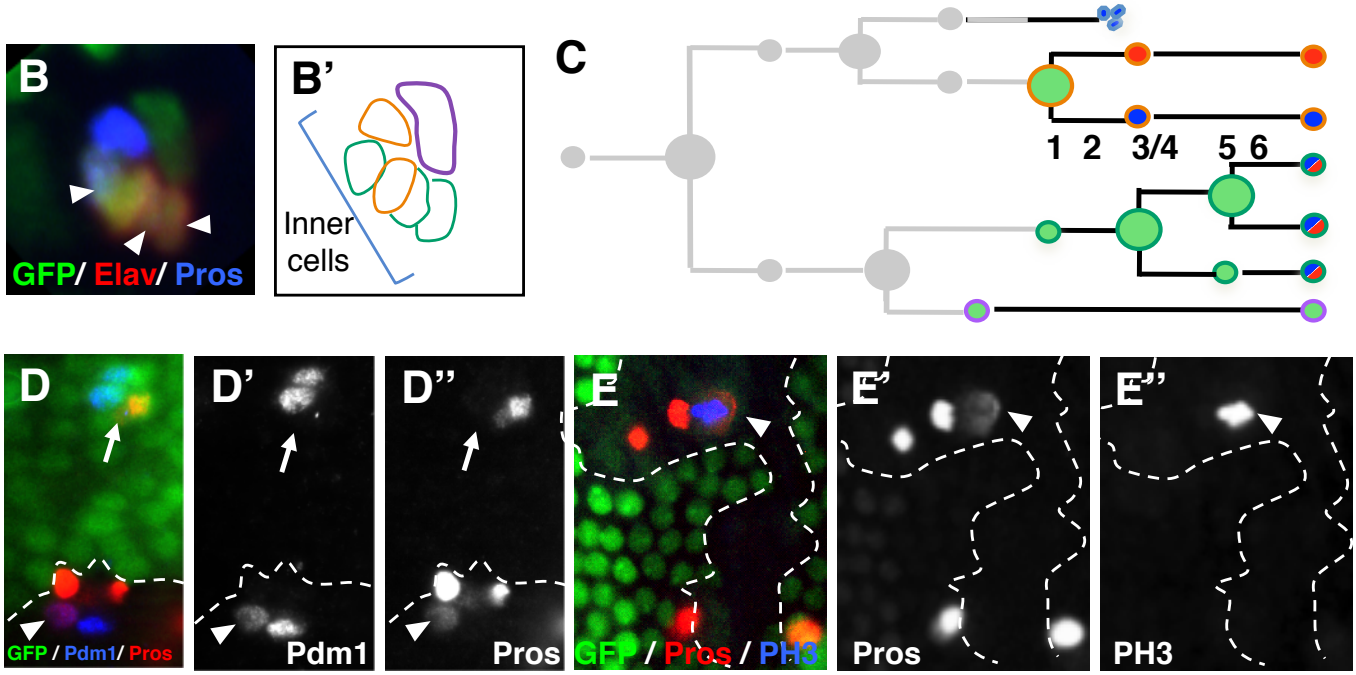

Figure 3. Presumptive Ttk69 mutant shaft cells undergo cell transformation toward inner precursor cells. (A, B, D, E) Ttk69 mutant clones detected by the absence of GFP (green). The white line shows the clonal border. (A) Combined 4D live imaging and lineage analysis showing extra divisions of the presumptive shaft cell. Representative frames (1-6) depicted in inverse fluorescence from a time-lapse recording of one Ttk69 mutant sensory organ at 20 h APF. The glial cell is outlined in blue, pIIb and its progeny in orange, the shaft cell and their daughters in green, and the socket cell in purple. Note that the presumptive shaft cell undergoes two rounds of division (frames 3 and 5). Note also the fragmentation of the apoptotic glial cell in frame 2. (B, B') Immunostaining and schematic representation of the same cluster after the time-lapse recording. Sensory cells are visualized by GFP expression (green). Cells adopting inner-cell fates are identified by anti-ELAV (red) and anti-Pros (blue) immunoreactivity. Note that three cells of the sensory organ are co-stained by anti-Pros and anti-ELAV antibodies (arrowheads). (C) Schematic view of the lineage shown in A. Cells are encircled using the same color code as in A and filled with same colors as in B. (D-D") Cousin-cousin cell fate transformation. Cells adopting outer or inner-cell fates were identified by the expression of Pdm1 (D' and blue in D) and Pros (D" and red in D) immunoreactivity, respectively. The arrowhead shows a Ttk69 mutant sensory organ in which a cell expresses both markers, a situation never observed in control sensory organs localized outside the Ttk69 clones (arrow). (E-E") Extra mitoses of inner cells revealed by PH3 immunoreactivity (E" and blue in E). Cells adopting an inner-cell fate were identified by Pros immunoreactivity (E' and red in E). Note that an extra division (arrowhead) was observed in a PH3 Pros-positive sensory organ.

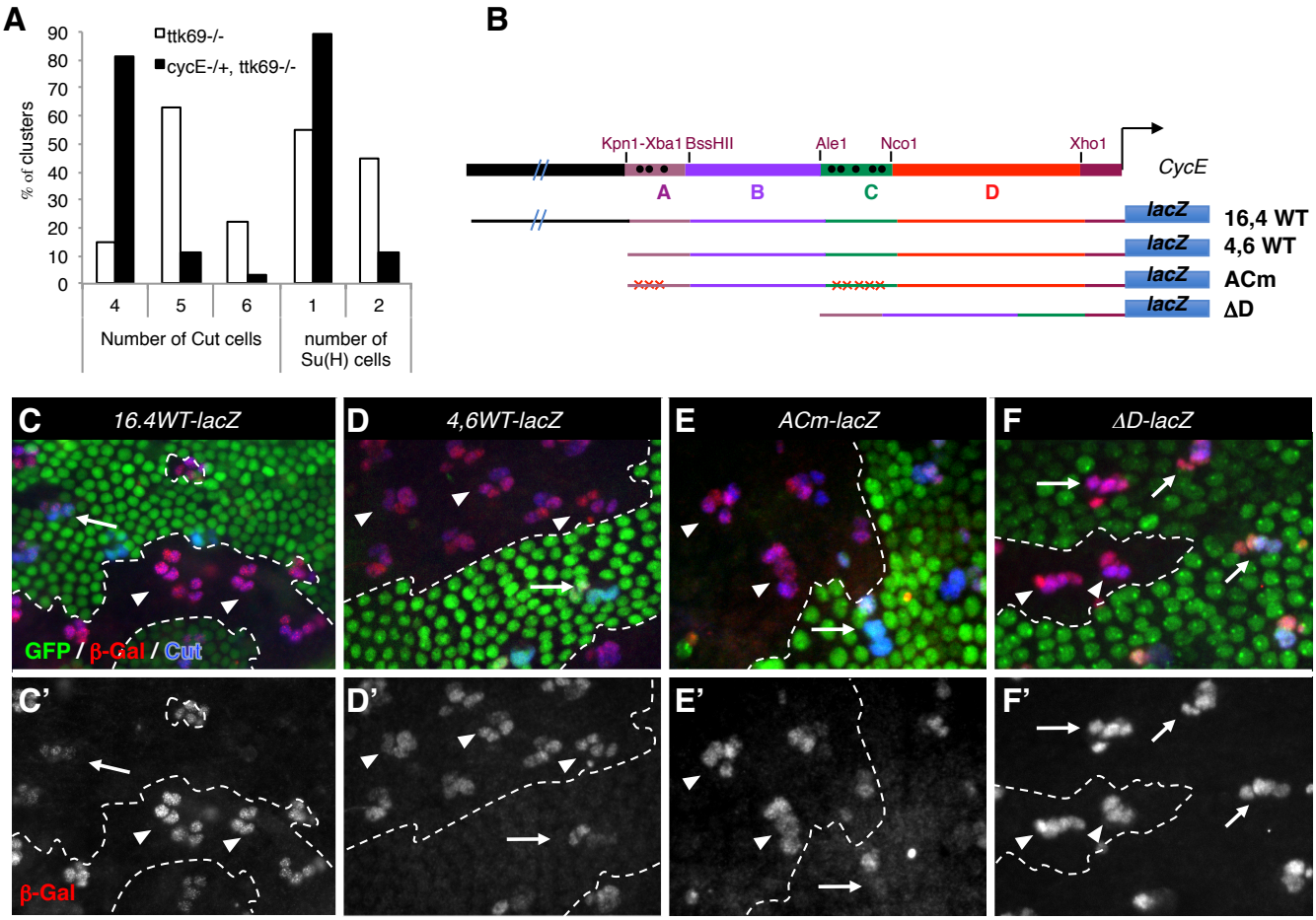

Figure 4. *cycE* expression is transcriptionally repressed by Ttk69. (A) Quantification of Ttk69 mutant sensory cells in $cycE^{+/+}$ or $cycE^{AR95/+}$ backgrounds. Histogram showing the percentage of Ttk69 mutant sensory organs harboring four to six Cut-positive cells (left) and one or two Su(H)-positive cells (right) in $cycE^{+/+}$ (white bars) or $cycE^{AR95/+}$ heterozygous (black bars) backgrounds. (B) Diagram of *cycE* transcriptional reporters aligned to the *cycE* promoter at the top. The localization of four specific regions (A to D) is depicted. Black dots indicate the localization of canonical AGGAC Ttk-binding sites. 16,4WT, *cycE* transcriptional reporter bearing the full-length *cycE* promoter; 4,6WT, bearing A to D regions; ΔCm, bearing A to D regions in which the eight AGGAC binding sites are mutated; and ΔD, bearing a deletion of the D region. (C, F) Expression pattern of the *16.4WT-lacZ* (C,C'), *4,6WT-lacZ* (D,D'), ΔCm-*lacZ* (E,E'), and *ΔD-lacZ* (F, F') *cycE* transcriptional reporters depicted in B in control sensory organs (located outside the clone, arrows) and Ttk69 mutant sensory organs (located inside the clone, arrowheads). Ttk69 clones were detected by the absence of GFP (green). White dashed lines indicate the border of the clone. Sensory cells were identified by Cut immunoreactivity (blue) and expression of *cycE* transcriptional reporters was revealed by β–Gal immunoreactivity (red and bottom panels). Note that β–Gal was ectopically expressed in control sensory organs when the D region was deleted (*ΔD-lacZ* construction, arrows).

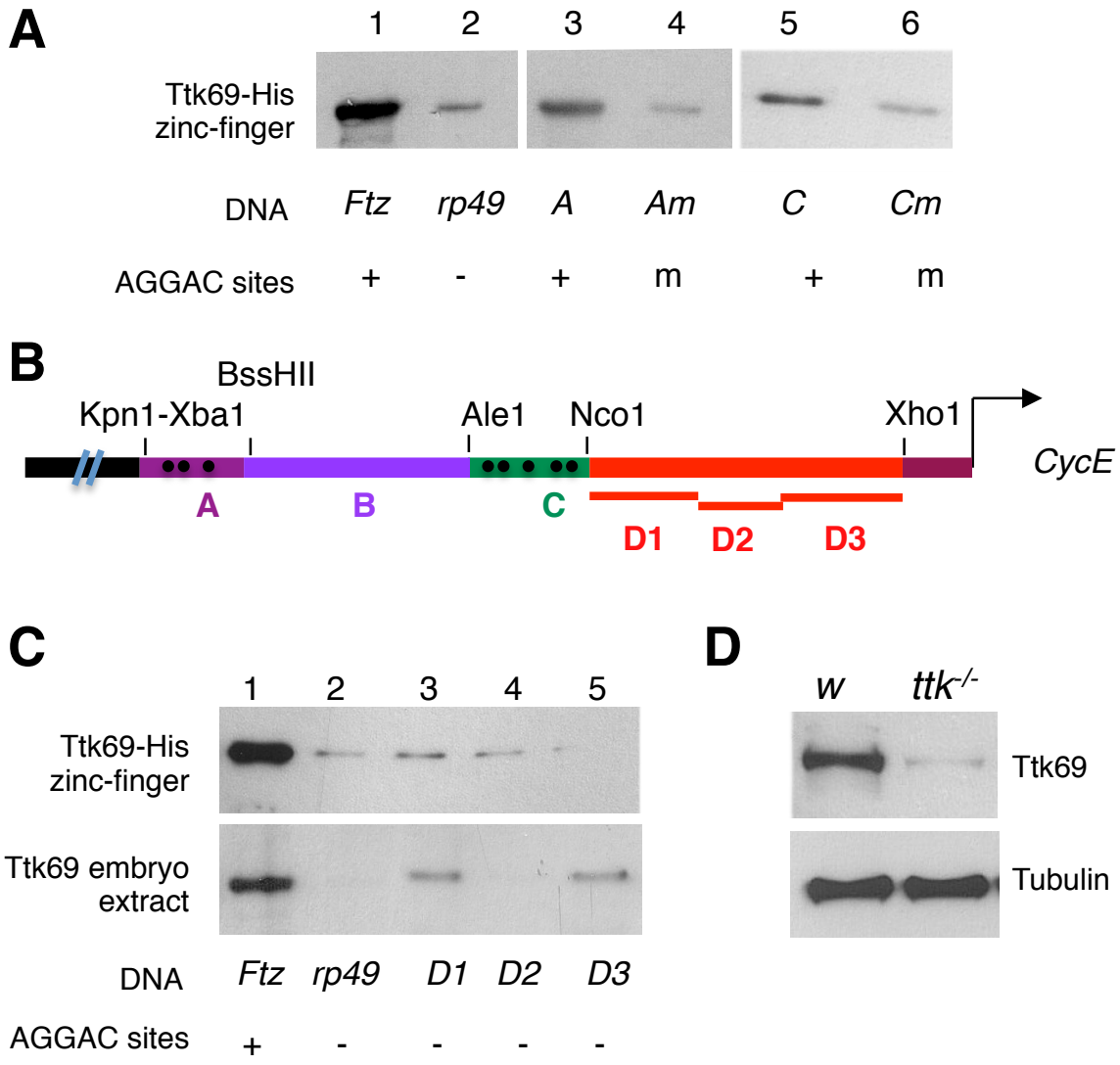

Figure 5. Ttk69 binds to the *cycE* promoter. (A) DNA-mediated Ttk69-His-zinc-finger pull-down assay. Magnetic beads were coated with: lane 1, *ftz* promoter as a positive control, bearing AGGAC binding sites; lane 2, *rp49* promoter as a AGGAC-free promoter negative control fragment; lanes 3 and 5, A and C regions, respectively, of the *cycE* promoter; lanes 4 and 6, Am and Cm regions, respectively, of the *cycE* promoter in which AGGAC binding sites were replaced by an unrelated TCGAC sequence (m). (B) Diagram of *cycE* promoter depicting the localization of the six specific regions (A to D3). Black dots indicate the localization of AGGAC binding sites. (C) DNA-mediated pull-down assay using Ttk69-his-zinc-finger (top) and whole Ttk69 protein from an embryo protein extract (bottom). Magnetic beads were coated with: lanes 1 and 2, as in B; and lanes 3, 4, and 5, the D1, D2, and D3 regions, respectively, of the *cycE* promoter. (D) Detection of Ttk69 protein. An immunoblot was prepared from a protein extract of one control (*white*) and one Ttk69 mutant embryo and probed with antibodies against Ttk69 and actin as a loading control.

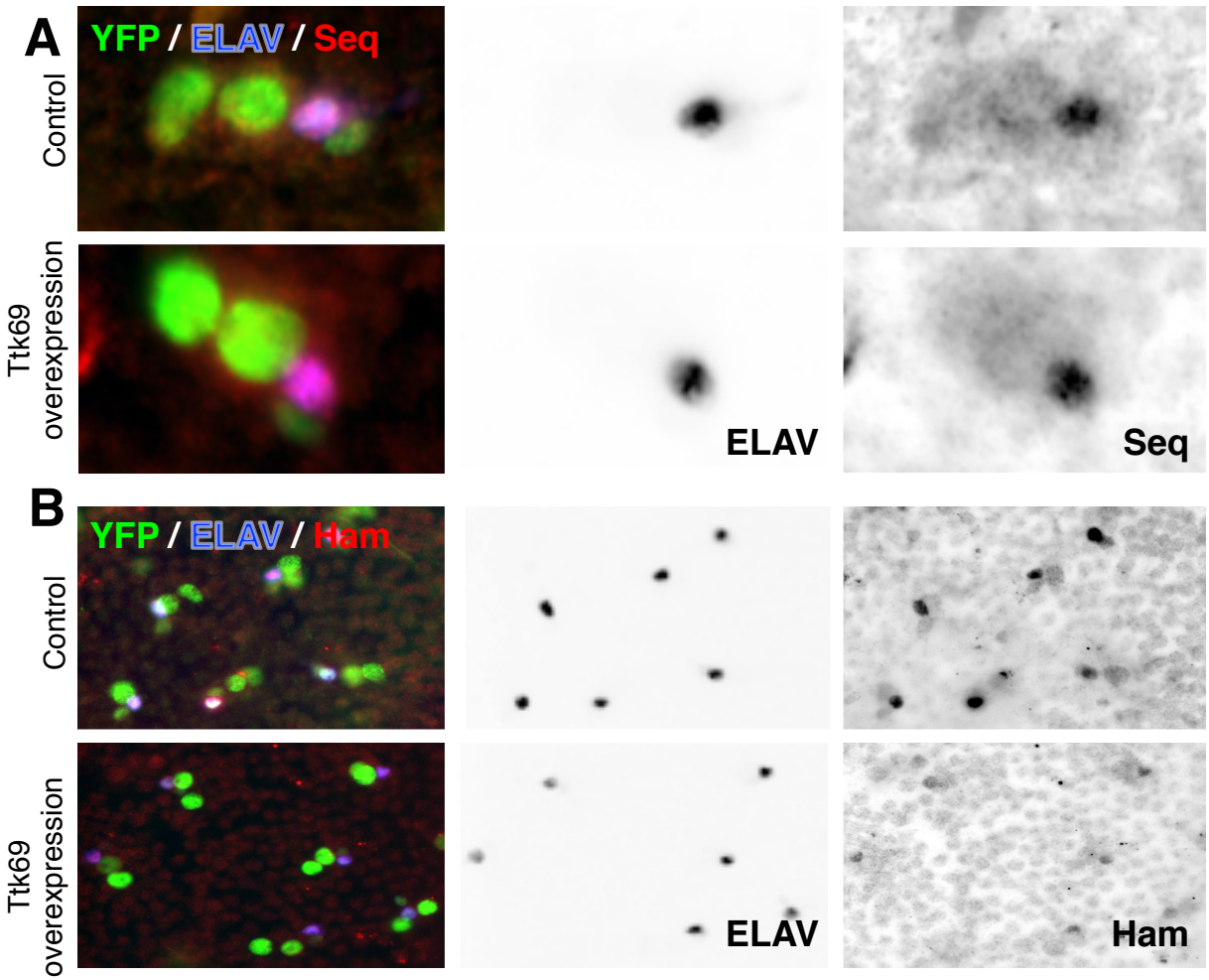

Figure 6. Ttk69 downregulates *hamlet* expression. (A, B) Over-expression of Ttk69 represses *hamlet* but not *sequoia* expression. Analysis of Seq (A) and Ham (B) protein accumulation after specific expression of Ttk69 in sensory cells. Sensory cells were visualized using YFP immunodetection (green). Neurons were identified by ELAV-specific expression (blue), Ham and Seq immunoreactivity (in red). Individual, ELAV (middle panels), Ham, and Seq channels (right panels) are shown in inverted color. Note that *ham* expression was markedly reduced. Note also that, under these conditions, no cell-fate transformation occurred as assessed by the stable expression of ELAV in neurons.

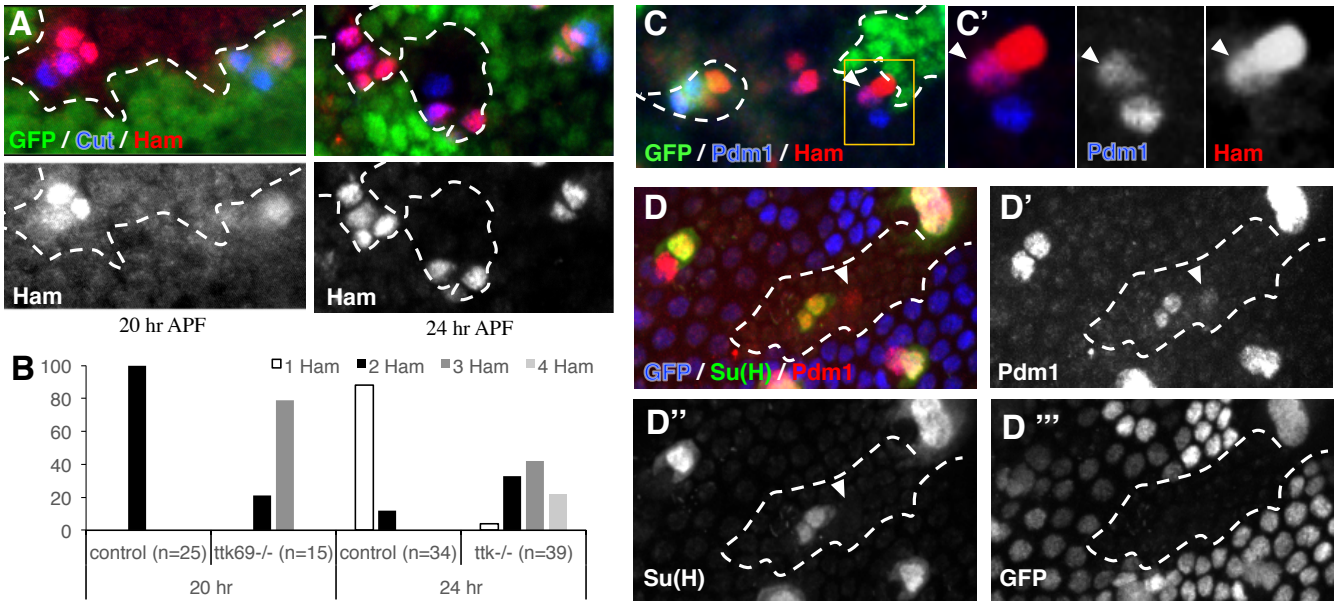

Figure 7: Ttk69 represses *hamlet* expression to maintain the non-neural cell fate.
(A) *ham* expression (red) in Ttk69 mutant sensory organs at 20 and 24 h APF. Ttk69 clones were detected by the absence of GFP (green), the white dashed lines indicating the border of the clone. Sensory cells were identified by Cut immunoreactivity (blue). (B) Histogram showing the percentage of sensory organs harboring one (white bars), two (black bars), three (dark grey bars), or four (pale grey bars) Ham-positive cells in control and Ttk69 mutant sensory organs at 20 and 24 h APF. (C) Cell transformation of a Pdm1-positive cell to a Ham-expressing cell. Ttk69 mutant sensory organs were identified by the absence of GFP in pupae at 22 h APF. Pdm1 and Ham immunoreactivity is shown in blue and red, respectively. The arrowhead indicates a cell positive for both, Pdm1 and Ham. (C') Higher magnification of the Ttk69-mutant cluster outlined in C. Merged and separate Pdm1 and Ham channels. (D) Recovery of shaft cells (Pdm1 positive, Su(H) negative) in Ttk69 clones in a *ham* heterozygous mutant background. Ttk69 mutant clones were detected by the absence of GFP in $ham^{+/-}$ pupae at 28 h APF (blue and D"'). Pdm1 (red and D') and Su(H) (green and D") immunoreactivity. Note the cell expressing only Pdm1, a landmark of shaft cells (arrowhead).

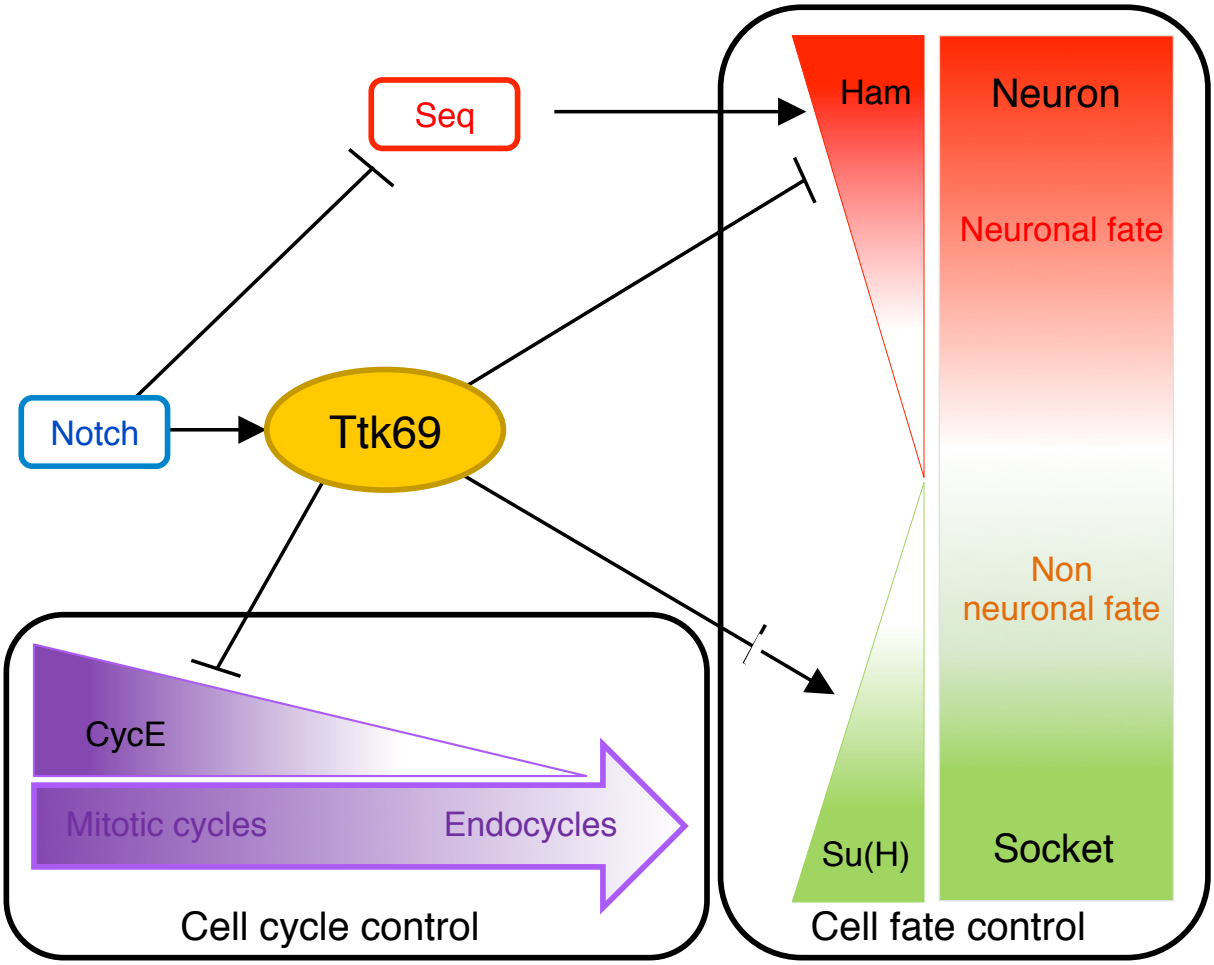

Figure 8. Ttk69 as a central node of a transcriptional regulatory network coordinating terminal cell fate acquisition and the arrest of cell proliferation. In response to N-pathway activation (Guo et al., 1995), Ttk69 (1) downregulates *cycE* expression inducing transition from a mitotic to endocycle mode of the cell cycle and (2) downregulates *ham* and upregulates *Su(H)* expression. Downregulation of *ham* expression prevents the acquisition of neural fate induced by the combined action of Seq and Ham (Andrews et al., 2009; Moore et al., 2004). Upregulation of *Su(H)* expression allows the terminal differentiation of socket cells.